Available online at www.sciencedirect.com
SCIENCE DIRECT®
International Journal of Mass Spectrometry 233 (2004) 87–98
International Journal of Mass Spectrometry
www.elsevier.com/locate/ijms

Theoretical study on the structures and dissociation channels of metal dications solvated by acetonitrile ligands

Chuanyun Xiao [a], Kendrick Walker [a], Frank Hagelberg [a,*], Ahmed M. El-Nahas [b]

[a] *Computational Center for Molecular Structure and Interactions, Department of Physics, Atmospheric Sciences and General Science, Jackson State University, Jackson, MS 39217, USA*
[b] *Chemistry Department, Faculty of Science, El-Menoufia University, Shebin El-Kom, Egypt*

Received 28 September 2003; accepted 18 November 2003
Dedicated to Professor Tilmann Märk on the occasion of his 60th birthday.

Abstract

The structures and dissociation channels of metal dications solvated by one or two acetonitrile ligands, $M^{2+}(CH_3CN)_n$ ($n = 1, 2$ for M = Be, and $n = 1$ for M = Mg, Ca, Fe, Cu, and Zn), were studied by density functional theory at the B3LYP/6-311+G(d, p) level. The dissociation processes studied include the loss of a neutral ligand, the dissociative electron transfer, and the cleavage of neutral and charged methyl (CH_3 and CH_3^+). For the diligated Be complex, the dissociative proton transfer is considered in addition to the processes indicated. The equilibrium structures of these complexes were found to be linear with the metal atom attached to the N-end of the CH_3CN ligands for all metals except Cu, for which the structure is slightly bent. The calculated dissociation energies indicate that the complexes are thermodynamically stable with respect to all considered processes for M = Be, Mg, Ca, and Fe, but are thermodynamically unstable with respect to the dissociative electron transfer process for M = Cu and Zn and to the cleavage of CH_3^+ for M = Cu. The energy barriers for the processes of dissociative electron transfer and the cleavage of CH_3^+ are determined for all units, which suggests that the $Zn^{2+}CH_3CN$ and $Cu^{2+}CH_3CN$ species are kinetically metastable with long lifetimes. The loss of neutral CH_3 is energetically unfavorable for all species. The loss of a neutral ligand is energetically unfavorable for all metals except Ca, where the loss of a neutral ligand is competitive with the dissociative electron transfer. The theoretical results agree well with available experimental observations.

Keywords: Multiply charged ions; Metal cations; Ion solvation; Dissociation; Stability

1. Introduction

Solvation of metal ions is a subject of strong and continuing interest. This can be largely attributed to the need of understanding metal ion coordination in various chemical environments. Particular attention has been paid lately to applications in the context of biological molecules [1,2]. In recent years, numerous research efforts have concentrated on the microsolvation in finite systems, since these systems can be conveniently studied stepwise by various mass spectrometric techniques [3,4] and are tractable by high-level quantum chemical theory. Thorough understanding of chemical processes generally benefits from their microscopic study in finite systems.

Although many of the important solvated metal ions in chemistry and biochemistry are doubly charged and can exist as stable species in solution, these units have not been experimentally accessible in the gas phase until recently. The difficulty in generating solvated metal dications experimentally arises from the large difference between the second ionization potential (IP_2) of a metal and the first IP (IP_1) of a ligand. The IP_1 of most common organic ligands lies in the range of 8–12 eV [5], while the IP_2 of almost all metal atoms (except alkaline earths) are above 12 eV. Therefore, in the absence of any stabilizing interaction, an encounter between a bare metal (M) dication and a neutral ligand (L) leads to immediate electron transfer followed by dissociation driven by Coulomb repulsion (or "Coulomb explosion") [6], namely, $M^{2+}L_n \rightarrow M^+L_{n-1} + L^+$. This hinders sequential ligation of multiply charged metal ions in the manner that is standard for singly charged ones—by passing through the vapor of a desired ligand species. Even the metal dications

* Corresponding author. Tel.: +1-601-979-3640; fax: +1-601-968-8623.
E-mail address: frank.d.hagelberg@ccaix.jsums.edu (F. Hagelberg).

1387-3806/$ – see front matter © 2004 Elsevier B.V. All rights reserved.
doi:10.1016/j.ijms.2003.11.017

with IP_2 below the ligand IP_1 that do not undergo electron transfer can often not be ligated by sequential addition, due to the existence of other competitive charge-separating dissociation channels, including dissociative proton transfer and intra-ligand cleavages [6–8]. Such problems exist in finite systems but disappear in solution since the Coulomb interaction in the latter is shielded by the dielectric environment. This raises the question for the minimum number of solvent molecules required to stabilize the $M^{2+}L_n$ complex and for the nature of the stabilization mechanism.

Several experimental techniques have been developed to successfully generate metal dications [9–11]. Most experimental work has concentrated on aqueous metal ions [8,9,12–17]. Except for hydrated ions, attention was mostly devoted to metal ions solvated by acetonitrile (CH_3CN) [18–24] and dimethyl sulfoxide (DMSO) [9,18,25]. Complexes involving a variety of other solvents were also successfully generated, such as ammonia, benzene, alcohols, acetone, ketones, ethers, and pyridine [17,19,26–31].

The generation and dissociation chemistry of doubly charged metal–acetonitrile complexes have been reported by several experimental groups [18–24]. Kohler and Leary [19,20] first investigated the low-energy fragmentation pathways of $M^{2+}(CH_3CN)_n$, where $n = 1$, 2 and M = Ca, Sr, Mn, and Co. Later, Seto and Stone [21] studied the dissociation of $Cu^{2+}(CH_3CN)_n$ with $n = 2$–4, while Stace and coworkers [22,23] observed the fragmentation of $M^{2+}(CH_3CN)_n$ with M = Mg, Cu, Ag, and Au for some sizes. Very recently, a comprehensive mass spectrometric study of metal dications solvated by acetonitrile was reported by Shvartsburg et al. [24], where the dissociation of $M^{2+}(CH_3CN)_n$ with M = Be, Mg, Ca, Sr, Ba, Fe, Co, Ni, Cu, Zn, and Cd was systematically examined. The observed dissociation pathways include dissociative electron and proton transfer processes, loss of neutral ligands, and heterolytic cleavage of CH_3^+.

Similar to the experimental studies, most theoretical investigations have been carried out for metal dications solvated by water [7,32–34]. Some theoretical efforts have also been made to analyze metal dications ligated with ammonia, formaldehyde, acetone, and DMSO [32,35,36]. These studies indicated that the interaction between M^{2+} and L is mainly electrostatic and that, for most of the studied monosolvated metal dications $M^{2+}L$, although the products $M^+ + L^+$ are lower in energy than $M^{2+} + L$, an avoided crossing of the $M^{2+} - L$ and $M^+ - L^+$ potential energy surfaces gives rise to a local minimum, corresponding to a sizable energy barrier in the adiabatic potential energy surface. These findings lead to the prediction that these species are kinetically metastable and thus experimentally detectable with sufficiently long lifetimes. Especially, the prediction of the existence of the $Cu^{2+}H_2O$ monomer has stimulated a lively discussion between theory [32] and experiment [15–17], and was finally confirmed by most recent experiments [16,17]. Therefore, high-level theory can provide valuable information to understand experimental observations related to the dissociation behavior of ligated dications, and guide further experimental work.

To the best of our knowledge, ab initio calculations of the metal–acetonitrile complexes were performed only for some neutral and singly charged species, including MCH_3CN and M^+CH_3CN (M = Al and alkaline metals) [37–40] and $Cu^+(CH_3CN)_n$ ($n = 1$–5) [41]. For the doubly charged species, $M^{2+}(CH_3CN)_n$, only a simple electrostatic model was applied to determine the n_{min} (the minimum number of ligands necessary to stabilize the metal dication) and n_{max} (at which the given $M^{2+}L_n$ complex is found with highest abundance) for M = Mg, Cu, Ag, and Au [22,23,29].

In this contribution, the equilibrium structures of $M^{2+}CH_3CN$ (M = Be, Mg, Ca, Fe, Cu, and Zn) and $Be^{2+}(CH_3CN)_2$, various dissociation products, the transition states that define the energy barriers for the charge-separating processes, and the energetic properties involved in all processes under consideration are systematically studied by a hybrid density functional theory procedure. The selected metals represent three types: alkaline earth metals (Be, Mg, Ca), magnetic (Fe), and nonmagnetic (Cu, Zn) transition metals. The considered dissociation pathways include dissociative electron transfer, loss of a neutral ligand, heterolytic cleavage of CH_3^+, and dissociative proton transfer [for $Be^{2+}(CH_3CN)_2$]. In addition, the cleavage of neutral CH_3 is considered for comparison with that of CH_3^+. We aim to arrive at a systematic theoretical understanding of related experimental observations in order to complement and guide experimental work.

The article is arranged as follows: the computational details are described in Section 2; the results are presented and discussed in Section 3, and our final conclusions are given in Section 4.

2. Computational details

The equilibrium geometries of $M^{2+}CH_3CN$ (M = Be, Mg, Ca, Fe, Cu, and Zn) and $Be^{2+}(CH_3CN)_2$, various dissociation products and related transition states, as well as the neutral and the cationic ligands, CH_3CN and CH_3CN^+, were fully optimized without symmetry constraints using the B3LYP hybrid density functional method in conjunction with the 6-311+G(d, p) basis set implemented in Gaussian 98 program [42]. The B3LYP density functional consists of a combination of Becke's three-parameter exchange functional (B3) [43] with Lee, Yang, and Parr's (LYP) correlation functional [44]. This method with similar or smaller basis sets has been applied successfully to study the structures and dissociation processes for the complexes of alkaline earth and transition metal dications ligated with H_2O, NH_3, acetone, and DMSO [32–36].

For complexes of all metals we considered, with the exception of Fe, the lowest possible spin multiplicity is assumed. For the Fe species and its dissociated products, all possible spins up to a septet state were considered and the

most stable structures found to correspond to a spin quintet state. To examine this prediction which involves a comparison between different electronic states of a transition metal atom containing species for possible sensitivity on the applied method, we subjected the unit $Fe^{2+}CH_3CN$ to an additional analysis, employing the Coupled Cluster method with single, double, and triple excitations [CCSD(T)]. Total energies were computed for $Fe^{2+}CH_3CN$ with all possible spin multiplicities up to the spin septet state and at the equilibrium structures obtained by optimization using the B3LYP method. In this comparison, the B3LYP and CCSD(T) procedures lead to very similar conclusions regarding the stability of the $Fe^{2+}CH_3CN$ species. Both methods yield the same order of stabilities within the considered sequence of spin multiplicities and thus single out the spin quintet state as the most stable one. The energy differences between adjacent spin states as obtained from B3LYP calculation, however, deviate within a range of 10–30% from the corresponding CCSD(T) values.

All structures reported have been verified to be local minima (no imaginary frequencies) or transition states (one imaginary frequency) on their respective potential energy surfaces by frequency analysis at the B3LYP/6-311+G(d, p) level.

In the theoretical investigation by Vitale et al. [41] on $Cu^+(CH_3CN)_n$ ($n = 1$–5), the zero-point energy (ZPE) and basis set superposition error (BSSE) corrections were estimated to be 0.5–1.0 and 0.1–0.7 kcal/mol, respectively, at the B3LYP/6-311+G(2d, 2p) level. Similarly, in a recent study [45] on Sc^{3+}DMSO at the B3LYP/6-311+G(d, p) level, we found that the ZPE and BSSE corrections were only 0.14 and 0.43%, respectively, of the metal–ligand dissociation energy. Therefore, the ZPE and BSSE corrections are ignored in the present work.

The atomic charges were calculated with the Natural Bond Orbital (NBO) program [46] as included in the Gaussian 98 package using the B3LYP/6-311+G(d, p) densities.

3. Results and discussion

In the following, we will first describe the structures of $M^{2+}CH_3CN$ (M = Be, Mg, Ca, Fe, Cu, and Zn) and $Be^{2+}(CH_3CN)_2$, their products in various dissociation processes as well as the transition states associated with charge separation, and then analyze the respective dissociation processes in terms of energetic properties.

3.1. Structures

The optimized geometries of $M^{2+}CH_3CN$ (M = Be, Mg, Ca, Fe, Cu, and Zn) and $Be^{2+}(CH_3CN)_2$, their products in various dissociation processes, and the transition states for dissociative electron transfer (TS1) and cleavage of CH_3^+ (TS2) are shown in Fig. 1, where the most significant geometric parameters are attached to the structures. More complete geometrical data and natural charges are documented in Table 1.

CH_3CN has trigonal symmetry with an N and a C atom attached to a methyl unit (CH_3) in a linear configuration. The optimized N–C, C–C, and C–H bond lengths in neutral CH_3CN are 1.153, 1.456, and 1.092 Å, respectively, and the C–C–H bond angle is 110.2° at the B3LYP/6-311+G(d, p) level. These geometric parameters compare well with those obtained by Imura et al. [37] at the MP2/6-311++G(d, p) level and by Vitale et al. [41] at the B3LYP/6-31G* level. For CH_3CN^+, the N–C and C–C bond lengths are elongated and shortened, respectively, by about 0.05 Å, while the C–H bond length and C–C–H angle are nearly unchanged. The calculated ionization potential and dipole moment for CH_3CN are 12.08 eV and 4.05 Debye, respectively, which agrees satisfactorily with the experimental data [24] of 12.2 eV and 3.9 Debye. Natural population analysis for CH_3CN indicates that the N atom and the C atom of the methyl group are negatively charged (−0.34 and −0.69e) while the C atom bonded to the N atom and the three H atoms adopt positive charges (0.29 and 0.25e).

In several recent calculations [37–41] on MCH_3CN (M = Al and alkaline earth metals) and $Cu^+(CH_3CN)_n$, the metal atoms were found to be bound preferentially to the N-end of the CH_3CN ligands. Therefore, we have attached the metal dications (M = Be, Mg, Ca, Fe, Cu, Zn) to the N-end of CH_3CN and the optimized structures are presented in Fig. 1. Except for Cu, the resulting CH_3CN–M complex adopts a linear shape. For $Cu^{2+}CH_3CN$, the linear conformation is a transition state and the relaxation leads to a slightly bent structure, with the bending angle Cu–N–C being 170.3°. The energy gain of the relaxation is as small as 0.8 kcal/mol. For $Fe^{2+}CH_3CN$, optimizations were performed in different spin conditions, ranging from singlet to septet. The most stable structure corresponds to a quintet, which is of the same spin multiplicity as free Fe^{2+}, and the spin polarization is localized on the Fe ion. Thus, the spin of Fe^{2+} ion is maintained in the $Fe^{2+}CH_3CN$ complex. For $Be^{2+}(CH_3CN)_2$, both linear and bent structures were considered and the two CH_3CN ligands were attached to Be with the same or opposite orientations of the H_3 subgroup. The bent structure was found to relax to the linear one after optimization and the conformation with opposite orientations of the H_3 subgroups is lower than that with equal orientations only by 0.02 kcal/mol. Therefore, different orientations of the ligands have little influence on the energy of the complex.

For all metal dications we considered, the N–C and C–C bond lengths of CH_3CN are slightly elongated and shortened, respectively, while the C–H bond length and the C–C–H angle are nearly unchanged upon attachment of the metal dication. The influence on the N–C and C–C bond lengths is smaller in $Be^{2+}(CH_3CN)_2$ than in $Be^{2+}CH_3CN$. As stated above, similar modifications in geometry are observed in CH_3CN^+, implying that some charge transfer might take place from CH_3CN to the metal in $M^{2+}CH_3CN$

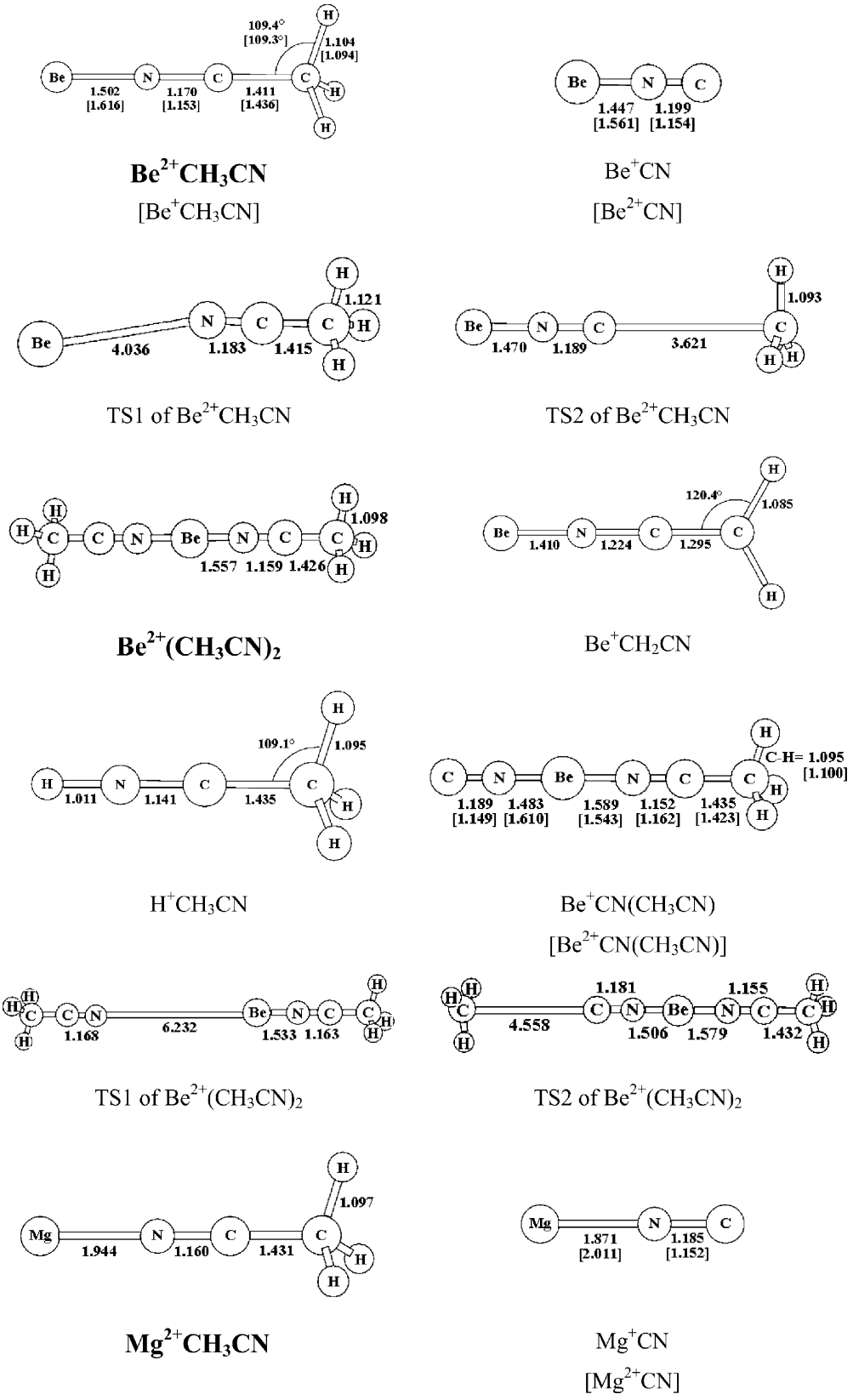

Fig. 1. Optimized structures (in Å and degree) of $M^{2+}CH_3CN$ (M = Be, Mg, Ca, Fe, Cu, Zn) and $Be^{2+}(CH_3CN)_2$, their products in various dissociation processes, and the transition states for dissociative electron transfer (TS1) as well as the cleavage of CH_3^+ (TS2), obtained at the B3LYP/6-311+G(d, p) level. For $Fe^{2+}CN$, bond lengths for spin sextet and quartet states are presented in brackets.

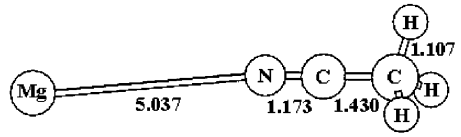

TS1 of $Mg^{2+}CH_3CN$

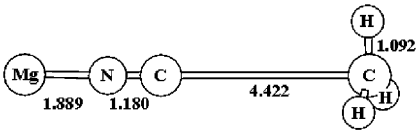

TS2 of $Mg^{2+}CH_3CN$

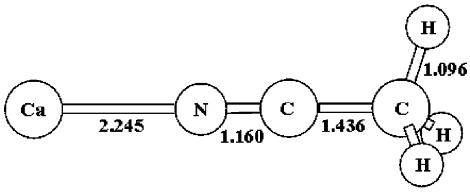

$Ca^{2+}CH_3CN$

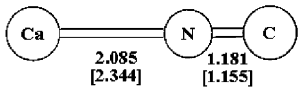

$Ca^{+}CN$

$[Ca^{2+}CN]$

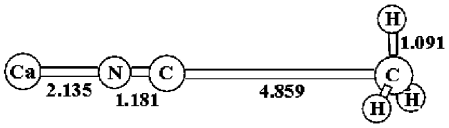

TS2 of $Ca^{2+}CH_3CN$

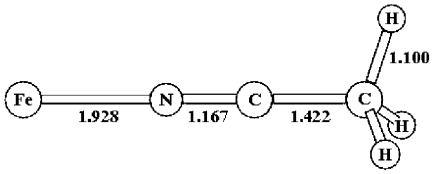

$Fe^{2+}CH_3CN$

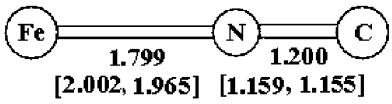

$Fe^{+}CN$

$[Fe^{2+}CN]$

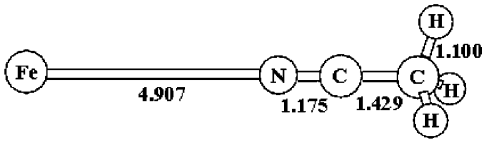

TS1 of $Fe^{2+}CH_3CN$

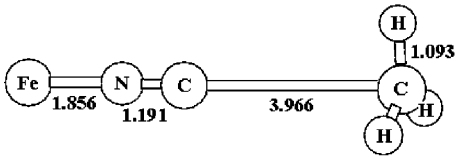

TS2 of $Fe^{2+}CH_3CN$

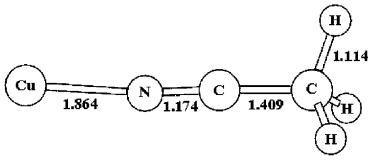

$Cu^{2+}CH_3CN$

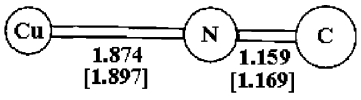

$Cu^{+}CN$

$[Cu^{2+}CN]$

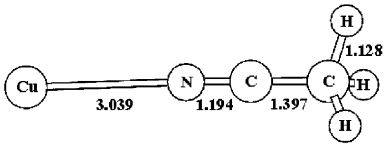

TS1 of $Cu^{2+}CH_3CN$

Fig. 1. (*Continued*)

and $Be^{2+}(CH_3CN)_2$. From Table 1, we see that there is charge transfer from CH_3CN to the metal ion in all species which proceeds more strongly in $Cu^{2+}CH_3CN$ than in other systems. As compared with pure CH_3CN, the solvation is accompanied by a considerable increase of the negative charge on the N atom and of the positive charge on the C atom next to N, while the charges on the atoms of the methyl unit are nearly unchanged. This indicates that the acetonitrile molecule is polarized at the N-end through metal dication attachment.

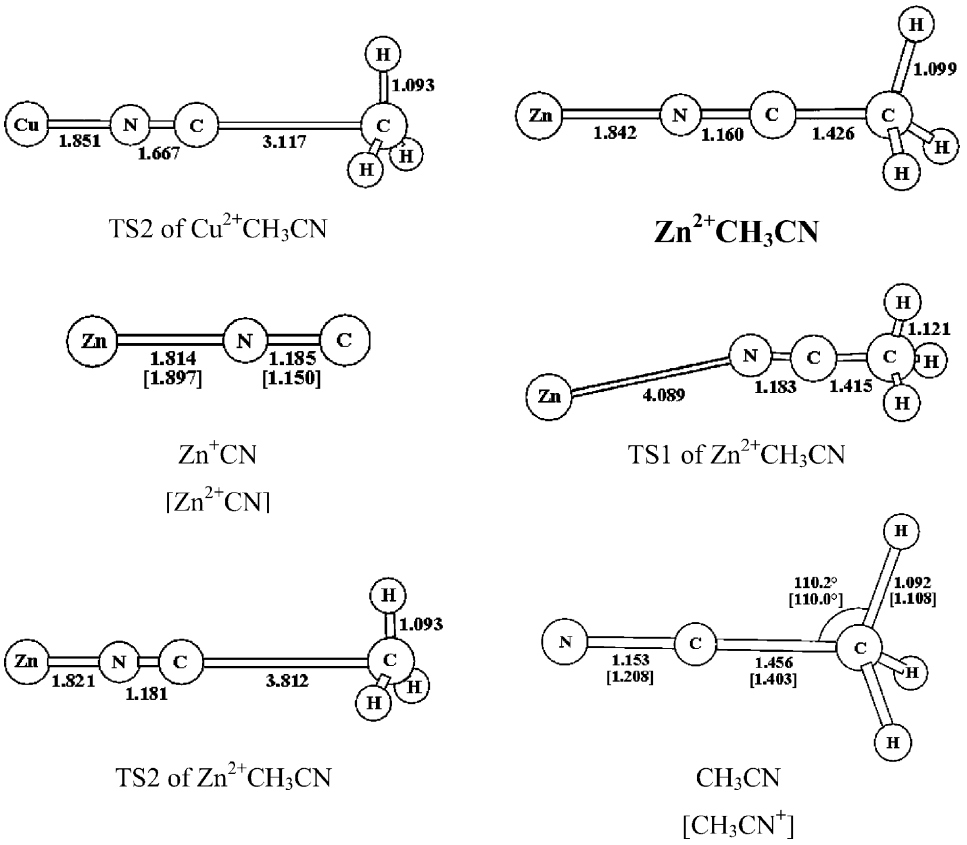

Fig. 1. (*Continued*).

Once the equilibrium structures of $M^{2+}CH_3CN$ (M = Be, Mg, Ca, Fe, Cu, and Zn) and $Be^{2+}(CH_3CN)_2$ are determined, their stabilities can be examined by subjecting these species to various dissociation reactions. For any $M^{2+}(CH_3CN)_n$ complex, the observed dissociation processes of $M^{2+}(CH_3CN)_n$ include [24]:

(a) Dissociative electron transfer (loss of CH_3CN^+)

$$M^{2+}(CH_3CN)_n \rightarrow M^{+}(CH_3CN)_{n-1} + CH_3CN^{+}$$

(b) Dissociative proton transfer (loss of H^+CH_3CN)

$$M^{2+}(CH_3CN)_n \rightarrow M^{+}CH_2CN(CH_3CN)_{n-2} + H^{+}CH_3CN$$

(c) Heterolytic cleavage of charged methyl (loss of CH_3^+)

$$M^{2+}(CH_3CN)_n \rightarrow M^{+}CN(CH_3CN)_{n-1} + CH_3^{+}$$

(d) Loss of neutral ligand

$$M^{2+}(CH_3CN)_n \rightarrow M^{2+}(CH_3CN)_{n-1} + CH_3CN$$

We have studied all of these processes. In addition, the following process was taken into account for a comparison with the cleavage of CH_3^+:

(e) Heterolytic cleavage of neutral methyl (loss of CH_3)

$$M^{2+}(CH_3CN)_n \rightarrow M^{2+}CN(CH_3CN)_{n-1} + CH_3$$

Charge separation is involved in processes (a–c), while processes (d) and (e) correspond to the loss of neutral ligands or ligand constituents. Since two ligands are involved in the dissociative proton transfer, this process can be studied only for $Be^{2+}(CH_3CN)_2$ within the scope of the systems considered here.

The structures for the products of all dissociation processes and the transition states for the charge-separating processes (a) and (c) of $M^{2+}CH_3CN$ and $Be^{2+}(CH_3CN)_2$ were determined (see Fig. 1 and Table 1). For $Ca^{2+}CH_3CN$, only TS2 was identified while TS1 does not exist. We will discuss this observation in Section 3.2 from the energetic point of view. For the cleavage of CH_3^+ or CH_3 in $Fe^{2+}CH_3CN$, a spin quintet was determined to be the ground state of Fe^+CN for the former process, while a sextet and a quartet were found to be the most competitive candidates of $Fe^{2+}CN$ unit for the latter. Although the quartet is lower than the sextet by 11.9 kcal/mol, this state is substantially spin contaminated, with $S(S+1) = 4.75$, and its Fe–N and N–C bond lengths are very close to those of the sextet. It appears likely that the sextet would emerge as lower in energy than the quartet if spin contamination could be eliminated from the latter. It should be noted that the qualitative conclusions drawn in the following subsection (Section 3.2) with respect to energetic properties are unaffected by the spin state used in the description of the dissociation behavior of $Fe^{2+}CH_3CN$, quartet or sextet.

Table 1
Geometric parameters (in Å and degree) and natural charges (Q) for $M^{2+}CH_3CN$ (M = Be, Mg, Ca, Fe, Cu, Zn) and $Be^{2+}(CH_3CN)_2$, their products in various dissociation processes, and the transition states for dissociative electron transfer (TS1) as well as cleavage of CH_3^+ (TS2), obtained at the B3LYP/6-311+G(d, p) level

	M–N[a]	N–C	C–C	M–N–C	N–C–C	C–C–H[b]	Q_M	Q_N	Q_C[c]
$Be^{2+}CH_3CN$	1.502	1.170	1.411	180.0	180.0	109.4	1.88	−1.01	0.83, −0.76
$Be^{+}CN$	1.447	1.199					1.83	−1.39	−0.56
$Be^{2+}CN$	1.561	1.154					1.90	−1.05	1.15
$Be^{2+}CH_3CN$, TS1	4.036	1.183	1.415	166.9	176.7	109.4	1.33	−0.17	0.50, −0.71
$Be^{2+}CH_3CN$, TS2	1.470	1.189	3.621	180.0	180.0	90.4	1.85	−1.29	0.47, 0.33
$Be^{2+}(CH_3CN)_2$	1.557	1.159	1.426	180.0	180.0	109.3	1.71	−0.84	0.74, −0.74
$Be^{+}CH_3CN$	1.616	1.153	1.436	180.0	180.0	109.3	0.95	−0.81	0.67, −0.73
$Be^{+}CH_2CN$	1.410	1.224	1.295	180.0	180.0	120.4	1.76	−1.32	0.52, −0.53
$H^{+}CH_3CN$	1.011	1.141	1.435	180.0	180.0	109.1	0.50	−0.40	0.70, −0.73
$Be^{+}CN(CH_3CN)$	1.589	1.152	1.435	180.0	180.0	109.3	1.69	−0.75	0.68, −0.73
	1.483[d]	1.189						−1.25	0.44
$Be^{2+}CN(CH_3CN)$	1.543	1.162	1.423	180.0	180.0	109.3	1.72	−0.87	0.77, −0.75
	1.610[d]	1.149						−0.90	1.02
$Be^{2+}(CH_3CN)_2$, TS1	1.533	1.163	1.420	180.0	180.0	109.3	1.59	−0.95	0.78, −0.75
	6.232[d]	1.168	1.439	180.0	180.0	109.3		−0.26	0.42, −0.71
$Be^{2+}(CH_3CN)_2$, TS2	1.579	1.155	1.432	180.0	180.0	109.3	1.70	−0.78	0.70, −0.73
	1.506[d]	1.181	4.558	180.0	180.0	90.2		−1.17	0.38, 0.33
$Mg^{2+}CH_3CN$	1.944	1.160	1.431	180.0	180.0	109.5	1.94	−0.85	0.69, −0.74
$Mg^{+}CN$	1.871	1.185					1.79	−1.19	0.40
$Mg^{2+}CN$	2.011	1.152					1.95	−0.92	0.96
$Mg^{2+}CH_3CN$, TS1	5.037	1.173	1.430	175.2	179.4	109.5	1.56	−0.24	0.46, −0.71
$Mg^{2+}CH_3CN$, TS2	1.889	1.180	4.422	180.0	180.0	90.1	1.86	−1.15	0.32. 0.33
$Ca^{2+}CH_3CN$	2.245	1.160	1.436	180.0	180.0	109.6	1.94	−0.78	0.63, −0.73
$Ca^{+}CN$	2.085	1.181					1.87	−1.19	0.32
$Ca^{2+}CN$	2.344	1.155					1.97	−0.84	0.89
$Ca^{2+}CH_3CN$, TS2	2.135	1.181	4.859	180.0	180.0	90.2	1.90	−1.12	0.30, 0.29
$Fe^{2+}CH_3CN$	1.928	1.167	1.422	180.0	180.0	109.5	1.80	−0.78	0.72, −0.75
$Fe^{+}CN$	1.799	1.200					1.54	−1.02	0.48
$Fe^{2+}CN$	2.002[e]	1.159					1.88	−0.88	1.00
	1.965[f]	1.155					1.84	−0.86	1.02
$Fe^{2+}CH_3CN$, TS1	4.907	1.175	1.429	180.0	180.0	110.2	1.55	−0.24	0.48, −0.72
$Fe^{2+}CH_3CN$, TS2	1.856	1.191	3.966	180.0	180.0	90.3	1.66	−1.02	0.39, 0.33
$Cu^{2+}CH_3CN$	1.864	1.174	1.409	170.3	176.1	109.9	1.49	−0.56	0.70, −0.73
$Cu^{+}CN$	1.874	1.159					1.08	−0.79	0.71
$Cu^{2+}CN$	1.897	1.169					1.52	−0.61	1.09
$Cu^{2+}CH_3CN$, TS1	3.039	1.194	1.397	177.8	179.9	109.7	1.11	−0.12	0.57, −0.72
$Cu^{2+}CH_3CN$, TS2	1.851	1.167	3.117	180.0	180.0	90.7	1.37	−0.79	0.48, 0.28
$Zn^{2+}CH_3CN$	1.842	1.160	1.426	180.0	180.0	109.3	1.84	−0.83	0.73, −0.75
$Zn^{+}CN$	1.814	1.185					1.56	−1.07	0.52
$Zn^{2+}CN$	1.897	1.150					1.88	−0.91	1.03
$Zn^{2+}CH_3CN$, TS1	4.089	1.183	1.415	166.6	176.6	109.3	1.34	−0.17	0.50, −0.71
$Zn^{2+}CH_3CN$, TS2	1.821	1.181	3.812	180.0	180.0	90.3	1.69	−1.05	0.39, 0.33
CH_3CN		1.153	1.456		180.0	110.2		−0.34	0.29, −0.69
CH_3CN^{+}		1.208	1.402		180.0	110.1		0.09	0.59, −0.75

[a] M is the metal or H atom attached to the N-end of CH_3CN.
[b] C–C–H is the angle related to the top H atom of the ligand. For $Be^{2+}(CH_3CN)_2$, the second C–C–H angle is associated with the bottom H atom of the second ligand (see Fig. 1).
[c] Charges for C atoms connected to N and H atoms, respectively.
[d] Geometric parameters and natural charges for atoms of the second ligand (the left one in Fig. 1).
[e] Spin sextet.
[f] Spin quartet, with strong spin contamination.

As seen in Fig. 1, the transition state TS1 for the cleavage of CH_3^+ of all species adopts a linear structure. For the transition state TS2 of the dissociative electron transfer process, the linear structure is identified only for $Fe^{2+}CH_3CN$ and $Be^{2+}(CH_3CN)_2$, while a bent structure is found for all other monoligated species $M^{2+}CH_3CN$ (M = Be, Mg, Cu, and Zn), with the M–N–C bending angle ranging from 166.6 to 177.8°. To elucidate the chemical reason for the bending of these structures, we plot the highest occupied molecular orbital (HOMO) for the representative species $Be^{2+}CH_3CN$

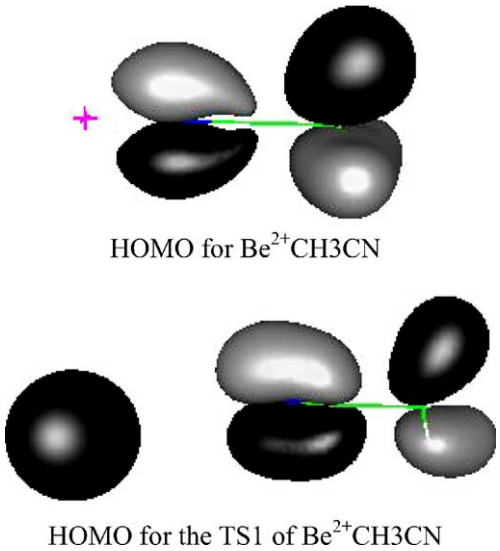

Fig. 2. The highest occupied molecular orbitals (HOMO) for $Be^{2+}CH_3CN$ and its transition state for the dissociative electron transfer process (TS1).

and its transition state TS1 in Fig. 2. Obviously, the N atom has a p component in both structures while the Be ion contributes little to the HOMO of the former but a large atomic s population to the HOMO of the latter. To maximize the Be–N interaction, the Be ion in TS1 moves towards the lower lobe of the p orbital of the N atom, resulting in a bent structure for TS1. Note that the effective charge on the Be ion in $Be^{2+}CH_3CN$ and in the TS1 configuration is 1.88 and 1.33e, respectively (see Table 1). Therefore, the Be ion exhibits a nearly closed shell in the former, but has 0.67 unpaired electrons in TS1 due to the charge transfer from the ligand to Be^{2+}. A similar analysis can be applied to other systems. Frequency calculations indicated that the only imaginary frequency for all of these transition states corresponds to the stretching mode between the two separated parts, confirming that the transition states with respect to the considered dissociation processes have been correctly identified.

It is worth while mentioning that in the transition state calculations a total charge (+2e) is imposed on the whole system. Therefore, the transition state TS1 can be understood to correspond either to the loss of CH_3CN^+ or neutral CH_3CN, and similarly, TS2 can be understood to correspond either to the loss of CH_3^+ or neutral CH_3, depending on the effective charge on the separated CH_3CN or CH_3 fragments. According to natural population analysis, the effective charge on the separated CH_3CN unit of TS1 ranges from +0.44 to +0.67e for the monoligated $M^{2+}CH_3CN$ species, and it reduces quickly from 0.67 to 0.32e as one goes from $Be^{2+}CH_3CN$ to $Be^{2+}(CH_3CN)_2$, implying that separation is possible for both CH_3CN and CH_3CN^+ and that the loss of a neutral ligand becomes more competitive with the increase of the number of ligands. In contrast, the effective charge on the separated CH_3 unit of TS2 is around +0.96e for all species. Therefore, no loss of neutral CH_3 will occur. Experimentally [24], the loss of CH_3CN, CH_3CN^+, and CH_3^+ were observed, while the loss of neutral CH_3 was not, in agreement with our findings. From Fig. 1, it is evident that the M–N and N–C bond lengths of TS2 are very similar to the corresponding bond lengths in the cleaved products M^+CN or $Be^+CN(CH_3CN)$, confirming that TS2 corresponds to the cleavage of CH_3^+ for each species. The energetic features of these four dissociation processes will be further discussed in the following subsection. Finally, we point out that all transition states exhibit a long distance (3.04–6.23 Å) between the two separated parts. Therefore, these transition state structures are all product-like, bearing the trace of the dissociation process.

3.2. Energetics

In this subsection, we will discuss the energetic properties of various dissociation processes and compare our respective conclusions with available experimental observations. The dissociation energies for various processes and the energy barriers defined by the transition states for the charge separation processes (a) and (c) of $M^{2+}CH_3CN$ and $Be^{2+}(CH_3CN)_2$ are displayed in Fig. 3. For all processes (a–e), the dissociation energy (D_e) is defined as the difference between the energy of the reactant complex (set to zero in Fig. 3) and the total energy of the dissociated products. Namely, $D_e = E(\text{products}) - E(\text{reactant complex})$.

Although Be, Mg, and Ca belong to the alkaline earth group, their second ionization potentials (IP_2) and hence dissociation behaviors differ markedly from each other. The calculated IP_2 of Be, Mg, and Ca are 18.60, 15.46, and 12.08 eV, respectively, which compare well with the experimental values of 18.2, 15.0, and 11.9 eV. The IP_2 of Be and Mg are larger than the first IP (IP_1) of CH_3CN (12.08 eV) while the calculated IP_2 of Ca matches the latter. It can be expected that the charge-transfer effect will be stronger in the Be than in the Mg-based species, and not appear in the Ca containing complex. Experimentally, both the electron and proton transfer processes were observed for $M^{2+}(CH_3CN)_n$ (M = Be, Mg) with $n \geq 1$ (electron transfer) or 2 (proton transfer) and the loss of neutral CH_3CN is not competitive for $n = 4$ (Be) or 3 (Mg) [24]. For $Ca^{2+}(CH_3CN)_n$, however, the loss of a neutral ligand is the primary fragmentation pathway, and neither the electron nor the proton transfer was observed for any size [24]. As for the heterolytic cleavage, the loss of CH_3^+ was observed for all of the three alkaline earth metals with $n \geq 1$, but no loss of neutral CH_3 was detected [24]. The calculated D_e values and energy barriers for $M^{2+}CH_3CN$ and $Be^{2+}(CH_3CN)_2$ in these processes are presented in Fig. 3. First of all, the calculated D_e values are positive for $M^{2+}CH_3CN$ and $Be^{2+}(CH_3CN)_2$ in all of the processes mentioned above. Therefore, all of these species are thermodynamically stable with respect to all the processes considered and the minimum number of ligands necessary to stabilize the alkaline earth metal dications is $n_{min} = 1$. The existence of energy barriers for charge separation processes, which have lower values of D_e than the processes

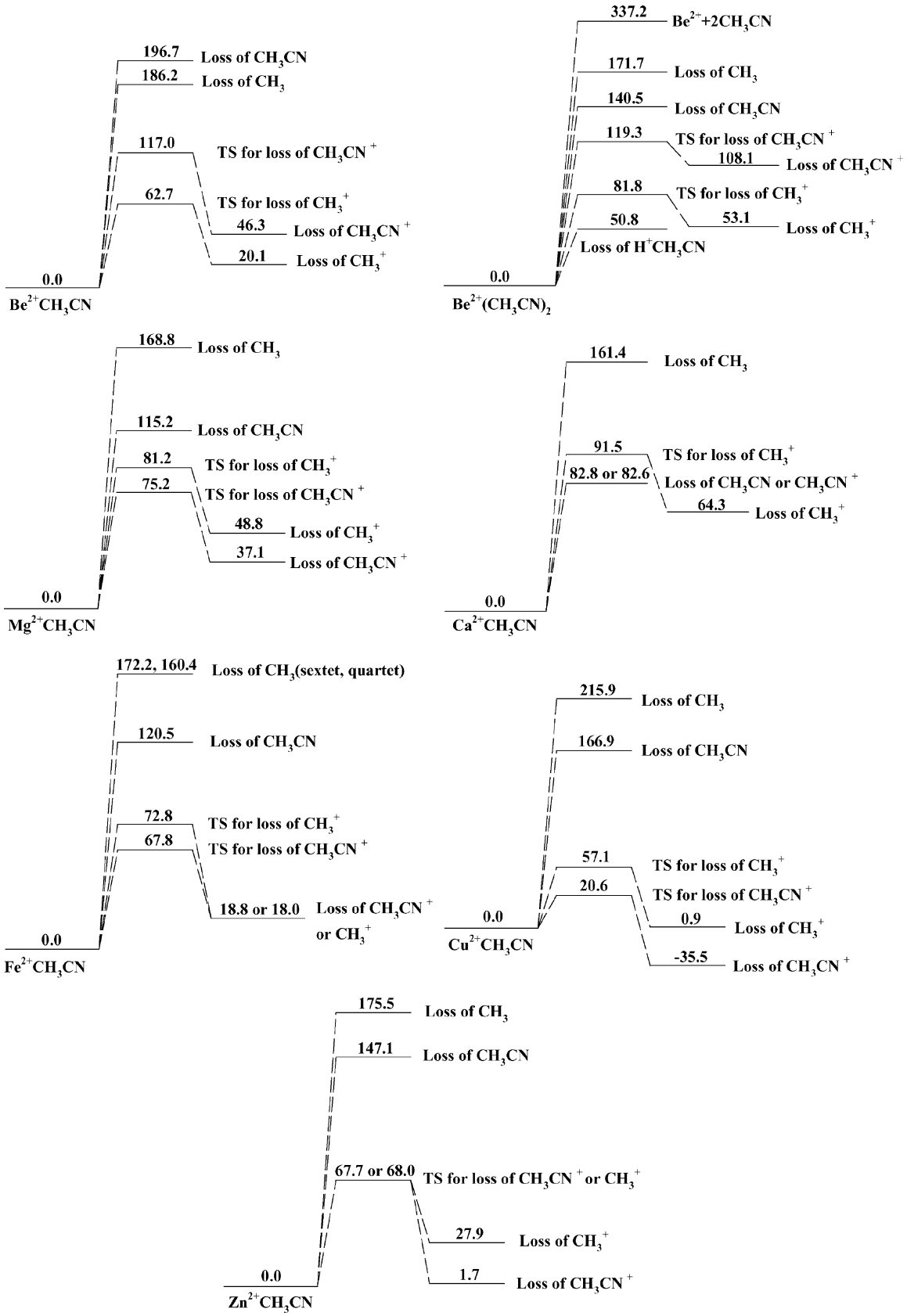

Fig. 3. Dissociation energies and energy barriers for various dissociation pathways of $M^{2+}CH_3CN$ (M = Be, Mg, Ca, Fe, Cu, Zn) and $Be^{2+}(CH_3CN)_2$, calculated at the B3LYP/6-311+G(d, p) level. For the cleavage of CH_3 in $Fe^{2+}CH_3CN$, results for the spin sextet and quartet states are both shown.

without charge reduction, further enhances the thermodynamical stability of these species. Secondly, the dissociation energy with respect to the loss of neutral CH_3CN is highest in $Be^{2+}CH_3CN$; in $Be^{2+}(CH_3CN)_2$ and $Mg^{2+}CH_3CN$, it drops lower than the value of D_e for the loss of CH_3 but still exceeds that for the loss of CH_3CN^+ and the related energy barrier. In $Ca^{2+}CH_3CN$, it adopts a value essentially equal to that for the loss of CH_3CN^+ (82.8 kcal/mol versus 82.6 kcal/mol). This means that the loss of neutral CH_3CN is energetically unfavorable in $Be^{2+}CH_3CN$, $Mg^{2+}CH_3CN$, and $Be^{2+}(CH_3CN)_2$, but competitive with the dissociative electron transfer in $Ca^{2+}CH_3CN$. It is worth mentioning that the identical dissociation energy for $Ca^{2+}CH_3CN$ with respect to neutral ligand loss and dissociative electron transfer processes results from the identity of the IP_1 of the ligand with the IP_2 of Ca, calculated at the B3LYP/6-311+G(d, p) level. Experimentally, since the IP_1 of the ligand (12.2 eV) is slightly larger than the IP_2 of Ca (11.9 eV), the dissociative electron transfer does not actually take place and the neutral ligand loss becomes the primary pathway. In fact, our efforts to determine the transition state (TS1) for the dissociative electron transfer of $Ca^{2+}CH_3CN$ failed consistently. Our results agree with the experimental observations that bare Be^{2+} was not observed, bare Mg^{2+} was observed in only small amounts, and the loss of neutral CH_3CN is the primary fragmentation pathway for the Ca-based complex. It should be noted that bare Be^{2+} and Mg^{2+} are the products of monoligated Be and Mg species in the process of neutral ligand loss. The anomalously high critical number $n_{crit} = 4$ (above which the loss of neutral ligand will become predominant) observed for the Be species in experiment can be attributed to the exceptionally high dissociation energy (196.7 kcal/mol) of $Be^{2+}CH_3CN$ for the loss of neutral ligand. Thirdly, for all of the three alkaline earth metals, the value of D_e for the loss of neutral CH_3 is much higher than that for the loss of CH_3^+. As a result, the cleavage of neutral CH_3 was observed for none of the alkaline earth metals in experiment. Finally, since the energy barrier for the loss of CH_3^+ is lower than that for the loss of CH_3CN^+ in $Be^{2+}(CH_3CN)_n$ ($n = 1, 2$), but the barriers associated with these two processes reverse their order in $Mg^{2+}CH_3CN$ and $Ca^{2+}CH_3CN$, the CH_3^+ cleavage process is expected to be more pronounced than the dissociation by electron transfer for the Be-based species but less so for the complexes containing Mg or Ca.

The remaining three metal atoms considered in the context of the work presented here, i.e., Fe, Cu, and Zn, belong to the 3d transition metal (TM) group. The calculated IP_2 of Fe, Cu, and Zn are 16.48, 20.85, and 18.38 eV, respectively, which agree within about 2% with the experimental data of 16.2, 20.3, and 18.0 eV. These IP_2 values are higher than the corresponding values of Mg and Ca and comparable to (for Fe, Zn) or even higher than (for Cu) that of Be. It follows that the charge-transfer effect will be much stronger in the TM–acetonitrile complexes than in the alkaline earth metal species, being strongest in the Cu and weakest in the Fe containing complex. Experimentally, the dissociative electron and proton transfer processes and the heterolytic cleavage of CH_3^+ were observed for all the three TM species with $n \geq 1$ (electron transfer and cleavage) or 2 (proton transfer), and bare TM^{2+} was observed only for TM = Fe [24]. In analogy to the alkaline earth metal species, the loss of neutral CH_3 was not observed in any TM–acetonitrile complexes [24]. The calculated dissociation energies and energy barriers for $TM^{2+}CH_3CN$ in various dissociation processes are shown in Fig. 3. For all TM species, the loss of neutral CH_3 is associated with the highest value of D_e among all processes, consistent with the absence of this process in experiment. The D_e for the loss of a neutral ligand is lower than that for the loss of neutral CH_3, but lies still much higher than those for the charge separation processes (loss of CH_3CN^+ and CH_3^+). Therefore, the neutral ligand loss is not competitive with the charge separation processes unless a substantial critical size is reached ($n_{crit} = 4$ for Fe, and 3 for Cu and Zn in Ref [24]). Furthermore, the bare TM^{2+} was observed for TM = Fe, but not for TM = Cu, and Zn [24], which may be correlated with the fact that the value of D_e for the neutral ligand loss of $TM^{2+}CH_3CN$ is the lowest for Fe in the TM = Fe, Cu, Zn series. The value of D_e for the charge-separating processes of $TM^{2+}CH_3CN$ decreases from TM = Fe to Zn and to Cu. The $Fe^{2+}CH_3CN$ species is thermodynamically very stable with respect to all dissociation processes considered here since the dissociation energies for the loss of CH_3CN^+ and CH_3^+ are both positive (18.8 and 18.0 kcal/mol, respectively), and the energy barriers for these two processes are very high (67.8 and 72.8 kcal/mol). For $Zn^{2+}CH_3CN$, the cleavage of CH_3^+ is endothermic with a considerably large D_e value of 27.9 kcal/mol, while the D_e value for the electron transfer process is positive but very small (1.71 kcal/mol), indicating that $Zn^{2+}CH_3CN$ is prone to dissociative electron transfer if no energy barrier exists. The energy barriers for these two charge separation processes were found to be nearly equal, amounting to 68.0 and 67.7 kcal/mol, respectively. Therefore, the $Zn^{2+}CH_3CN$ species is expected to be kinetically stable with respect to the electron transfer process, with a long lifetime. For $Cu^{2+}CH_3CN$, the cleavage of CH_3^+ exhibits a positive but small D_e (0.88 kcal/mol) while the electron transfer process is strongly exothermic with a negative D_e of −35.5 kcal/mol. Therefore, the $Cu^{2+}CH_3CN$ species is thermodynamically unstable with respect to both the CH_3^+ cleavage and the electron transfer processes. Confirmation of the $Cu^{2+}CH_3CN$ complex depends on the existence and height of the energy barriers for these two processes, which has proved to be the most challenging task involved in the work presented here. The transition states for these two processes were eventually obtained and the activation barriers were calculated to be 57.1 and 20.6 kcal/mol, respectively. These barriers are high enough to prevent $Cu^{2+}CH_3CN$ from spontaneous charge separation. From Fig. 3, it is realized that the energy barriers for $Cu^{2+}CH_3CN$ are lowest among all complexes compared,

indicating that $Cu^{2+}CH_3CN$ is the least stable species considered here.

4. Conclusions

In this contribution, the structures and dissociation channels of $M^{2+}CH_3CN$ (M = Be, Mg, Ca, Fe, Cu, and Zn) and $Be^{2+}(CH_3CN)_2$ complexes were studied by density functional theory at the B3LYP/6-311+G(d, p) level. The dissociation processes studied include the loss of a neutral ligand, the dissociative electron transfer, and the cleavage of neutral and charged methyl units (CH_3 and CH_3^+). For the diligated Be complex, the dissociative proton transfer is considered in addition to the above processes. The results obtained can be summarized as follows:

(1) The equilibrium structures for complexes of all metals except Cu are determined to be linear. For the Cu complex, a slightly bent structure is identified. The metal atom is attached to the N-end of CH_3CN in all species.
(2) The dissociated products and the dissociation energies for these complexes were determined for all processes considered. For the complexes of all metals except Ca, the dissociation energies for the loss of neutral ligand and CH_3 are considerably higher than for the corresponding charge separation processes. Therefore, neutral ligand loss or intra-ligand cleavage is energetically unfavorable for these complexes. For the Ca-based species, the dissociation energies for the neutral ligand loss and the electron transfer process are identical and the two processes therefore compete. For the charge separation process, the calculated dissociation energies are positive for complexes of all alkaline earth metals and Fe, indicating that these complexes are thermodynamically stable with respect to charge transfer. The dissociation energies of the electron transfer process for $Zn^{2+}CH_3CN$ and the cleavage of CH_3^+ for $Cu^{2+}CH_3CN$ are positive but very small, and turn out to be negative for the electron transfer process of $Cu^{2+}CH_3CN$. Therefore, the $Cu^{2+}CH_3CN$ and $Zn^{2+}CH_3CN$ complexes are thermodynamically unstable with respect to these processes.
(3) The transition states for the dissociative electron transfer and the CH_3^+ cleavage of $M^{2+}CH_3CN$ (M = Be, Mg, Ca, Fe, Cu, and Zn) and $Be^{2+}(CH_3CN)_2$ were determined and the related energy barriers were computed. The energy barriers were found to be sizable for all species, enhancing the stability of complexes with M = Be, Mg, Ca, and Fe, and making the complexes with M = Zn and Cu kinetically metastable with long lifetimes. The theoretical results agree well with available experimental observations.

An extension of the present research effort to other transition metals and to higher numbers of ligands is currently planned.

Acknowledgements

This work was supported in part by the National Science Foundation through the Grants HRD-9805465, NSF-0132618, and DMR-0304036, and in part by the Army High Performance Computing Research Center under the auspices of Department of the Army, Army Research Laboratory under Cooperative Agreement No. DAAD 19-01-2-0014. The authors thank Dr. Alexandre A. Shvartsburg for helpful discussions.

References

[1] K.D. Karlin, Science 261 (1993) 701.
[2] P.E.M. Siegbahn, M.R.A. Bloomberg, Chem. Rev. 100 (2000) 421.
[3] A.W. Castleman, K.H. Bowen, J. Phys. Chem. 100 (1996) 12911.
[4] J.M. Lisy, Int. Rev. Phys. Chem. 16 (1997) 267.
[5] R.R. Wright, N.R. Walker, S. Firth, A.J. Stace, J. Phys. Chem. A 105 (2001) 54.
[6] K.J. Spears, F.C. Fehsenfeld, J. Chem. Phys. 56 (1972) 5698.
[7] M. Beyer, E.R. Williams, V.E. Bondybey, J. Am. Chem. Soc. 121 (1999) 1565.
[8] A.A. Shvartsburg, K.W.M. Siu, J. Am. Chem. Soc. 123 (2001) 10071.
[9] P. Jayaweera, A.T. Blades, M.G. Ikonomou, P. Kebarle, J. Am. Chem. Soc. 112 (1990) 2452.
[10] M.P. Dobson, A.J. Stace, Chem. Commun. 1533 (1996).
[11] D. Schröder, H. Schwarz, J. Phys. Chem. A 103 (1999) 7385.
[12] Z.L. Cheng, K.W.M. Siu, R. Guevremont, S.S. Berman, J. Am. Soc. Mass Spectrom. 3 (1992) 281.
[13] S.E. Rodriguez-Cruz, R.A. Jockusch, E.R. Williams, J. Am. Chem. Soc. 120 (1998) 5842.
[14] S.E. Rodriguez-Cruz, R.A. Jockusch, E.R. Williams, J. Am. Chem. Soc. 121 (1999) 1986.
[15] A.J. Stace, N.R. Walker, R.R. Wright, S. Firth, Chem. Phys. Lett. 329 (2000) 173.
[16] J.A. Stone, D. Vukomanovic, Chem. Phys. Lett. 346 (2001) 419.
[17] D. Schröder, H. Schwarz, J. Wu, C. Wesdemiotis, Chem. Phys. Lett. 343 (2001) 258.
[18] Z.L. Cheng, K.W.M. Siu, R. Guevremont, S.S. Berman, Org. Mass Spectrom. 27 (1992) 1370.
[19] M. Kohler, J.A. Leary, J. Am. Soc. Mass Spectrom. 8 (1997) 1124.
[20] M. Kohler, J.A. Leary, Int. J. Mass Spectrom. Ion Processes 162 (1997) 17.
[21] C. Seto, J.A. Stone, Int. J. Mass Spectrom. Ion Processes 175 (1998) 263.
[22] N. Walker, M.P. Dobson, R.R. Wright, P.E. Barran, J.N. Murrell, A.J. Stace, J. Am. Chem. Soc. 122 (2000) 11138.
[23] N. Walker, R.R. Wright, P.E. Barran, J.N. Murrell, A.J. Stace, J. Am. Chem. Soc. 123 (2001) 4223.
[24] A.A. Shvartsburg, J.G. Wilkes, J.O. Lay, K.W.M. Siu, Chem. Phys. Lett. 350 (2001) 216.
[25] A.A. Shvartsburg, J.G. Wilkes, J. Phy. Chem. A 106 (2002) 4543.
[26] U.N. Anderson, G. Bojesen, Int. J. Mass Spectrom. Ion Processes 153 (1996) 1.
[27] A.J. Stace, N.R. Walker, S. Firth, J. Am. Chem. Soc. 119 (1997) 10239.
[28] B.J. Hall, J.S. Brodbelt, J. Am. Soc. Mass Spectrom. 10 (1999) 402.
[29] N.R. Walker, R.R. Wright, A.J. Stace, J. Am. Chem. Soc. 121 (1999) 4837.
[30] M. Peschke, A.T. Blades, P. Kebarle, J. Am. Chem. Soc. 122 (2000) 10440.
[31] A.A. Shvartsburg, J.G. Wilkes, Int. J. Mass Spectrom. 225 (2003) 155.

[32] A.M. El-Nahas, N. Tajima, K. Hirao, Chem. Phys. Lett. 318 (2000) 333; 329 (2000) 176.
[33] A.M. El-Nahas, Chem. Phys. Lett. 345 (2001) 325.
[34] A.M. El-Nahas, Chem. Phys. Lett. 348 (2001) 483.
[35] A.M. El-Nahas, Chem. Phys. Lett. 365 (2002) 251.
[36] J.A. Stone, T. Su, D. Vukomanovic, Int. J. Mass Spectrom. 216 (2002) 219.
[37] K. Imura, T. Kawashima, H. Ohoyama, T. Kasai, J. Am. Chem. Soc. 123 (2001) 6367.
[38] F. Bouchard, V. Brenner, C. Carra, J.W. Hepburn, G.K. Koyanagi, T.B. McMahon, G. Ohanessian, M. Peschke, J. Phys. Chem. A 101 (1997) 5885.
[39] K. Ohshimo, H. Tusnoyama, Y. Yamakita, F. Misaizu, K. Ohno, Chem. Phys. Lett. 301 (1999) 356.
[40] E.M. Cabalerio-Lago, M.A. Rios, Chem. Phys. 254 (2000) 11.
[41] G. Vitale, A.B. Valina, H. Huang, R. Amunugama, M.T. Rodgers, J. Phys. Chem. 105 (2001) 11351.
[42] M.J. Frisch, G.W. Trucks, H.B. Schlegel, G.E. Scuseria, M.A. Robb, J.R. Cheeseman, V.G. Zakrzewski, J.A. Montgomery Jr., R.E. Stratmann, J.C. Burant, S. Dapprich, J.M. Millam, A.D. Daniels, K.N. Kudin, M.C. Strain, O. Farkas, J. Tomasi, V. Barone, M. Cossi, R. Cammi, B. Mennucci, C. Pomelli, C. Adamo, S. Clifford, J. Ochterski, G.A. Petersson, P.Y. Ayala, Q. Cui, K. Morokuma, D.K. Malick, A.D. Rabuck, K. Raghavachari, J.B. Foresman, J. Cioslowski, J.V. Ortiz, B.B. Stefanov, G. Liu, A. Liashenko, P. Piskorz, I. Komaromi, R. Gomperts, R.L. Martin, D.J. Fox, T. Keith, M.A. Al-Laham, C.Y. Peng, A. Nanayakkara, C. Gonzalez, M. Challacombe, P.M.W. Gill, B.G. Johnson, W. Chen, M.W. Wong, J.L. Andres, M. Head-Gordon, E.S. Replogle, J.A. Pople, Gaussian 98, Revision A.9, Gaussian, Inc., Pittsburgh, PA, 1998.
[43] A.D. Becke, J. Chem. Phys. 98 (1993) 5648.
[44] C. Lee, W. Yang, R.G. Parr, Phys. Rev. B 37 (1988) 785.
[45] C. Xiao, F. Hagelberg, A.M. El-Nahas, A density-functional study on the structures, stabilities and dissociation pathways of $Sc3^{+}(DMSO)_n$ complexes ($n=1$–6), J. Phys. Chem. (submitted for publication).
[46] J.E. Carpenter, F. Weinhold, J. Mol. Struct. (Theochem.) 169 (1988) 41.